Pergamon

SCIENCE DIRECT®

Bioorganic & Medicinal Chemistry 11 (2003) 5035–5043

BIOORGANIC & MEDICINAL CHEMISTRY

Analysis of Structural Features of Bis-Quaternary Ammonium Antimicrobial Agents 4,4′-(α,ω-Polymethylenedithio)bis (1-alkylpyridinium Iodide)s Using Computational Simulation

Kazuto Ohkura,[a,b] Akiko Sukeno,[a] Keiko Yamamoto,[a] Hideaki Nagamune,[a] Takuya Maeda[a] and Hiroki Kourai[a,*]

[a]*Department of Biological Science and Technology, Faculty of Engineering, University of Tokushima, 2-1 Minamijosanjima-cho, Tokushima 770-8506, Japan*
[b]*Bioagricultural Science, Nagoya University, Furo-cho, Chikusa-ku, Aichi 464-8601, Japan*

Received 19 June 2003; accepted 28 August 2003

Abstract—The bis-quaternary ammonium compounds (QACs) consisted of two identical alkylpyridinium rings and a bridge structure linking the rings to each other. The QACs have a methylene bridge except for 4DCABP-P,12 which has a phenyl ring as a bridge. These bis-QACs are as follows; amide type: *N,N′*-tetramethylenebis(1-dodecyl-4-carbamoylpyridinium iodide) (4BCAP-4,12), *N,N′*-hexamethylenebis(1-decyl-4-carbamoylpyridinium iodide) (4BCAP-6,10), anti-amide type: 4,4′-(1,4-tetramethylenedicarbonyldiamine)bis(1-decylpyridinium iodide) (4DCABP-4,10), 4,4′-(1,4-tetramethylenedicarbonyldiamine)bis (1-dodecylpyridinium iodide) (4DCABP-4,12), 4,4′-(1,4-phenyldicarbonyldiamine)bis(1-dodecylpyridinium iodide) (4DCABP-P,12), ester type: 4,4′-(1,6-hexamethylenedioxydicarbonyl)bis(1-dodecylpyridinium iodide) (4DOCBP-6,12), thioether type: 4,4′-(1,6-hexamethylenedithio)bis(1-octylpyridinium iodide) (4DTBP-6,8). From the investigation of the relationship between the median lethal dose (LD_{50}) and the minimum inhibitory concentration (MIC) of these compounds, 4DTBP-6,8 as a disinfectant, seems to be very safe for human cells. The global minimum of 4DTBP-6,8 were searched and 1125 conformers obtained. The solvation free energy (dGW) of nine samples, which were extracted from these 1125 conformers, was calculated and two minimum points of dGW were observed. In the conformer–energy analysis of four types of model bridge-molecule, the thioether type bridge indicated a gradual energy increment, while the other three (amide, anti-amide, ester) types indicated an energy jump point in their profiles. Then we considered that the delicate balance between hydrophobicity and structural feature in the bridge-region of 4DTBP-6,8 molecule seemed to be related to its safety antibacterial activity.

Introduction

Hospital infections, such as Methicillin-resistant *Staphylococcus aureus* (MRSA), are a social problem. The safe extermination of bacteria is very important to human health care. Quaternary ammonium compounds (QACs), such as benzalkonium chloride or cetylpyridinium chloride, have been used widely in clinical, food production and health care. These compounds seem to be safer than the disinfectants such as chlorine and glutaraldehyde, but they have irritating and cytotoxic effect on human cells or tissues such as keratinocytes, fibroblasts, cornea and respiratory mucosa.[1–4] We designed and synthesized a series of antimicrobial mono-QACs, and studied their bactericidal mechanism.[5–12] In these mono-QACs, a quantitative structure activity relationship with molecular hydrophobicity,[13,14] adsorbability,[15] surface activity,[16] electron density of the ammonium nitrogen,[17,18] or bacteriostatic activity was previously reported.[5]

On the other hand, the synthesis and the antimicrobial activities of bis-QACs have been reported by Devinsky et al.,[16,19] and Pavlikova-Moricka et al.[20] Kourai et al. reported that *N,N′*-dialkyl-γ,γ′-dipyridinium diiodides (PP-*n*,*n*) exhibited stronger antibacterial activity than mono-QACs.[9] In addition, the antimicrobial characteristics of PP-*n*,*n*, with two similar alkyl chains, were comparable to those of QACs with two different alkyl chains. The synthesis and the antimicrobial or anti-tumor effects

*Corresponding author. Fax: +81-88-656-9148; e-mail: kourai@bio.tokushima-u.ac.jp

0968-0896/$ - see front matter © 2003 Elsevier Ltd. All rights reserved.
doi:10.1016/j.bmc.2003.08.027

of polymeric QACs have also been reported.[21–23] Previously, we reported the synthesis of four types of novel bis-QACs (Fig. 1): (1) amide type [4BCAP-4,12: *N,N′*-tetramethylenebis(1 - dodecyl - 4 - carbamoylpyridinium iodide), 4BCAP-6,10: *N,N′*-hexamethylenebis(1-decyl-4-carbamoylpyridinium iodide)], (2) anti-amide type [4DCABP - 4,10: 4,4′ - (1,4 - tetramethylenedicarbonyldiamine)bis(1-decylpyridinium iodide), 4DCABP-4,12: 4,4′ - (1,4 - tetramethylenedicarbonyldiamine)bis(1 - dodecylpyridinium iodide), 4DCABP-P,12: 4,4′-(1,4-phenyldicarbonyldiamine)bis(1-dodecylpyridinium iodide)], (3) ester type [4DOCBP-6,12: 4,4′-(1,6-hexamethylenedioxydicarbonyl)bis(1-dodecylpyridinium iodide)], and (4) thioether type [4DTBP-6,8: 4,4′-(1,6-hexamethylenedithio)bis(1-octylpyridinium iodide)]. These bis-QACs consisted of two identical alkylpyridinium rings and a bridge structure linking the rings to each other. The bis-QACs have a methylene bridge except for 4DCABP-P,12 which has a phenyl ring as a bridge.

In the present study, we aimed to compare the cytotoxicity of these compounds with widely distributed antimicrobial benzalkonium chloride (Bz), especially regarding cytotoxicity to human keratinocytes (normal human epidermal keratinocytes of neonatal foreskin: NHEK(F)) and human fibroblast (normal human fibroblast cell lines: NB1RGB) which would most frequently come into contact with such antiseptics if the bis-QACs are included in any soap or cleaning liquid. We also tested the effect on human normal erythrocytes and T-cell lymphoma (JM) which is a model cell line for lymphocytes, with regard to the situation where a user of the antimicrobials has any injury on the skin resulting in QACs in the blood stream thereby contacting blood cells in addition to contacting skin cells. From the investigation of the relationship between 50% of lethal dose (LD_{50}) and minimal inhibitory concentration (MIC) of these compounds, 4DTBP-6,8 seems to be very safe disinfectant for human cells. Then we analyzed the structural features of 4DTBP-*m,n* conformers using CONFLEX, and calculated the solvation free energy (dGW). The value of dGW is considered one of the parameters for hydrophobicity. We obtained dGW using the molecular orbital calculations as described.[24–27] Moreover we obtained the energy-conformer profiles of four types of modeled bridge-molecules (amide, anti-amide, ester, thioether type), and will discuss the effect of bridge feature both on antibacterial activity and safety.

Results

Acute cytotoxic effect of bis-QACs on human cells

We examined the acute cytotoxic effect of these amide type, anti-amide type, ester type, thioether type bis-QACs (Fig. 1) on human normal epidermal keratinocytes from neonatal foreskin (NHEF(K)) and a normal skin fibroblast cell line (NB1RGB), representing the main components of the epidermis and the dermis. Moreover, blood cells, which can come into contact with these QACs when the skin is damaged or injured, namely human normal erythrocytes and JM cells as a model for the lymphocytes, were also used (Table 1).

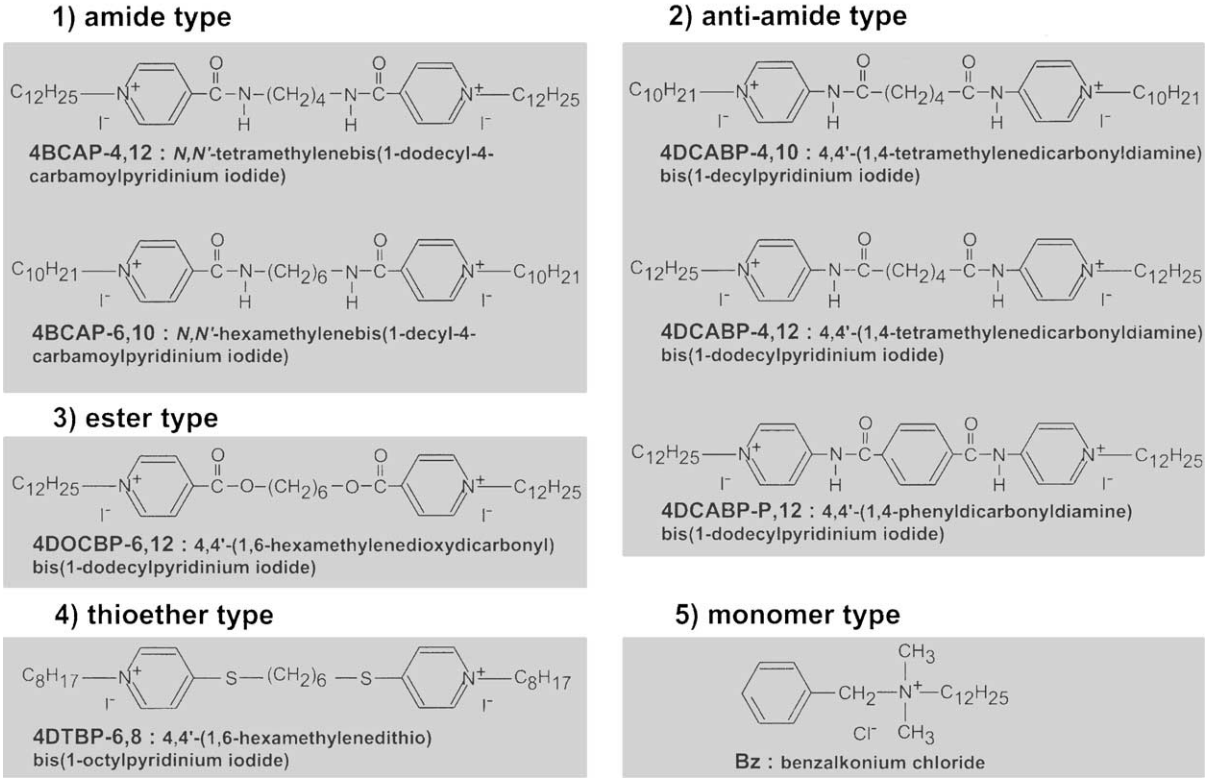

Figure 1. Structures of bis-quaternary ammonium compounds (QACs). Four types of QACs: amide type (1), anti-amide type (2), ester type (3), thioether type (4). Monomer type (5).

Table 1. Acute cytotoxic effect of QACs on human cells

QAC	LD50 in human cells (μM)[a]			
	NHEK(F)	NB1RGB	Erythrocyte	JM
Bz	19±2	54±4	74±5	65±5
4BCAP-4,12	13±3	40±3	6±2	20±3
4BCAP-6,10	13±2	31±3	18±2	22±4
4DCABP-4,10	42±6	52±4	6±1	23±3
4DCABP-4,12	16±5	53±3	12±2	30±4
4DCABP-P,12	34±4	50±4	22±3	46±3
4DOCBP-6,12	13±2	52±3	11±3	50±5
4DTBP-6,8	8±2	48±4	25±4	41±4

Bz, benzalkonium chloride.
[a]Means±SD ($n=2$).

All tested QACs completely killed the exposed cells in a concentration range of $10^{-5}\sim10^{-4}$ M. NHEK(F) cells were the most susceptible to all QACs, although the susceptibility to the QACs of the other three cell types (NB1RGB, erythrocyte, JM) tested varied for each QAC. Amide type QACs (4BCAP-4,12, 4BCAP-6,10) had a similar degree of cytotoxicity toward NHEK(F). The LD_{50} of 4BCAP-4,12 was lower than that of 4BCAP-6,10 in erythrocyte and JM. In the anti-amide type 4DCABP-4,12, the LD_{50} toward NHEK(F) was lower than the other two compounds (4DCABP-4,10, 4DCABP-P,12), and the value was 16±5 μM. The cytotoxicity (LD_{50}) of 4DOCBP-6,12 (ester type) and 4DTBP-6,8 (thioether type) toward NHEK(F) were 13+2 and 8+2 μM, respectively. Benzalkonium chloride (Bz) apparently seems to be a relatively mild reagent among the antimicrobials tested, but antimicrobial activity and the cytotoxicity side-effect must be comprehensively evaluated. Thus, regarding a typical compound from each type of QACs, we compared the minimum inhibitory concentration (MIC) as the index for antimicrobial activity.

Most susceptible and resistant strains, and the minimal inhibitory concentration (MIC) are shown in Table 2.

Table 2. Most susceptible and resistant strains to QACs

QAC	Strain	MIC (μM)
Bz	*B. subtilis* IFO3134	4.2
Bz	*P. mirabilis* IFO3849	205
4BCAP-4,12	*P. vulgaris* ATCC13315	0.4
4BCAP-4,12	*K. pneumoniae* ATCC13883	12.5
4DCABP-4,12	*P. vulgaris* ATCC13315	<0.1
4DCABP-4,12	*P. aeruginosa* (all three strains)	12.5
4DOCBP-6,12	*S. aureus* IFO12732	3.3
4DOCBP-6,12	*P. aeruginosa* ATCC27583	80.0
4DTBP-6,8	*B. subtilis* IFO3134	<0.2
4DTBP-6,8	*P. mirabilis* IFO3849	10.0

Most susceptible and resistant strains was *B. subtilis* IFO3134 and *P. mirabilis* IFO3849 to benzalkonium chloride (Bz); *P. vulgaris* ATCC13315 and *K. pneumoniae* ATCC13883 to 4BCAP-4,12; *P. vulgaris* ATCC13315 and all three stains (Experimental) of *P. aeruginosa* to 4DCABP-4,12; *S. aureus* IFO12732 and *P. aeruginosa* ATCC27583 to 4DOCBP-6,12; *B. subtilis* IFO3134 and *P. mirabilis* IFO3849 to 4DTBP-6,8, respectively.

The MIC range of 4BCAP-4,12 was 0.4–12.5 μM, similar to the level of LD_{50} in human cells (Table 1). Then cytotoxicity of 4BCAP-4,12 for human cells, especially NHEK(F), erythrocyte, and JM, should be concerned with complete disinfection. The MIC of 4DCABP-4,12 (<0.1–12.5 μM) was the same degree to the LD_{50} in NHEK(F), erythrocyte, JM; thus, a cytotoxic effect was feared. The MIC to *Pseudomonas aeruginosa* ATCC27583 (80 μM) of 4DOCBP-6,12 was higher than the LD_{50} value in four types of human cells, therefore, this compound was not useful. 4DTBP-6,8 had a lower MIC range (<0.2–10.0 μM) than LD_{50} in NB1RGB, erythrocyte, JM, and was most useful among the compounds tested in the present study. Surprisingly, the MIC of Bz was 4.2–205 μM, and the range was higher than the LD_{50} in all human cells, the worst in this regard among the compounds tested.

Effect of alkyl-bridge (*m*) and -chain (*n*) length in the 4DTBP-*m*,*n* molecule on bacteriostatic activity

4DTBP-*m*,*n* molecules consisted of two identical alkylpyridinium rings with a bridge structure linking the rings to each other have a methylene bridge (Fig. 2). Next, we examined the effect of alkyl-chain (*n*) length on the bacteriostatic activity. In 4DTBP-3,n derivatives, alkyl-chain (*n*) length affected the minimum inhibitory concentration (MIC) to *Escherichia coli* K12 W3110 (Fig. 2A). The MIC was unchanged up to 12 (*n*) of the alkyl-chain length, and MIC increased at a chain length of 14–18 (*n*). In 4DTBP-4,*n*,-6,*n*,-8,*n* and-10,*n* derivatives, the MIC was almost unchanged at 8–12 (*n*), and increased at an alkyl-chain length of 14–18 (*n*) as well as for 4DTBP-3,*n* (Fig. 2B–E). Thus 8 (*n*) of alkyl-chain length induced the lowest MIC in bacteriostasis.

Effect of the alkyl-bridge (*m*) length in the 4DTBP-*m*,8 molecule on the MIC is indicated in Figure 2F. The MIC decreased at a 3–6 alkyl-bridge (*m*) but the MIC value increased at 8 (*m*) of bridge length. From these results, an alkyl-bridge of 6 (*m*) and an alkyl-chain length of 8 (*n*) (4DTBP-6,8) was the most useful antimicrobial agent among the bis-QACs, which had been examined in the present study.

Global minimum search and solvation free energy calculation for 4DTBP-*m*,8 derivatives

We performed the global minimum search for 4DTBP-6,8 using CONFLEX (Fujitsu Ltd., Japan), and obtained 1125 conformers. The energy profile of these conformers is indicated in Figure 3. We extracted nine conformers (samples 1–9), that showed the holding process of 4DTBP-6,8. The energy level was −0.56 (sample 1) to 12.65 (sample 9) kcal/mol. To analyze this holding process theoretically, their solvation free energies (dGW), which are considered as one of the parameters for hydrophobicity, were obtained by molecular orbital calculations as previously described (a lower dGW value indicates higher hydrophobicity).[25–27] The correlation between the dGW values and the holding process (samples 1–9, Fig. 3) of 4DTBP-6,8 are shown in Fig. 4 (open circles in right panel). Two dGW

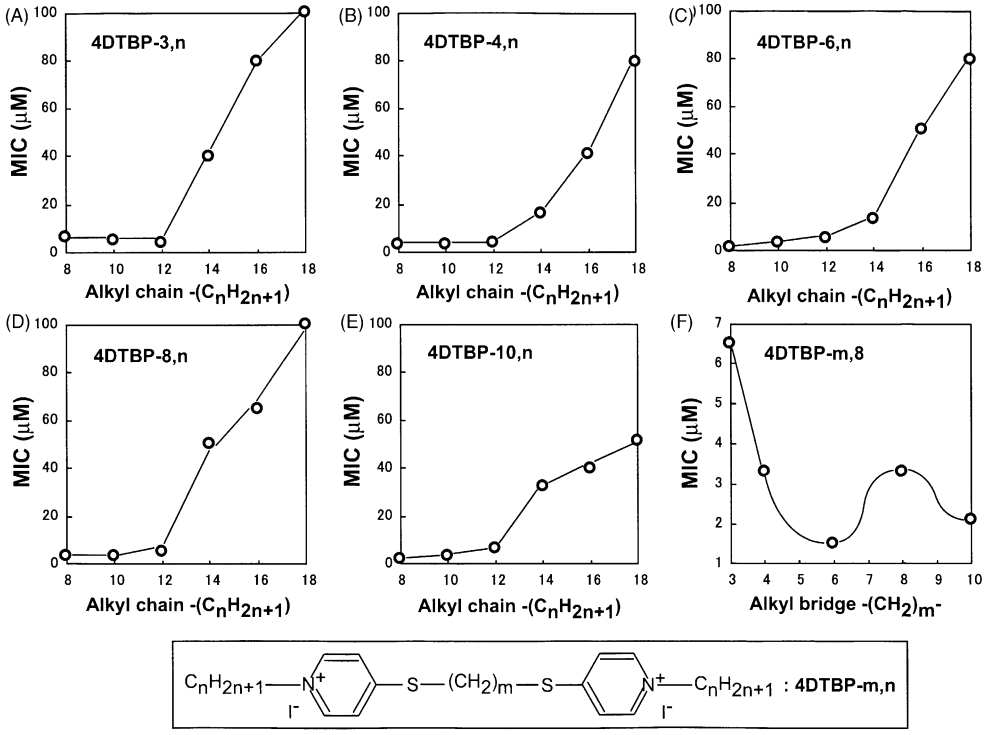

Figure 2. Effect of alkyl-bridge (*m*) and alkyl-chain (*n*) length on minimal inhibitory concentration (MIC) in *E. coli*. The effect of alkyl-chain length on MIC in 4DTBP-3,*n* (A), -4,*n* (B), -6,*n* (C), -8,*n* (D) and -10,*n* (E) derivatives, respectively. The relationship between the alkyl-bridge length and the MIC in the 4DTBP-*m*,8 molecule (F).

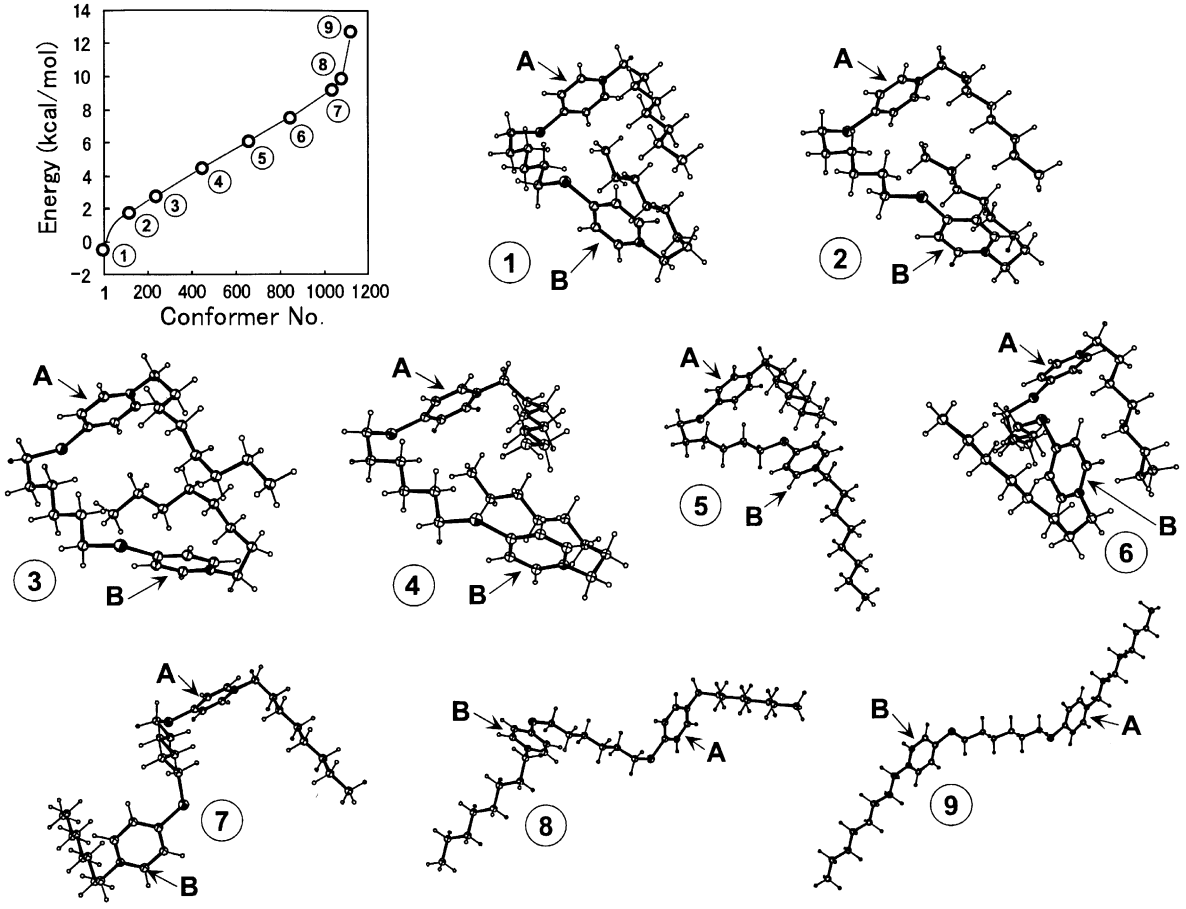

Figure 3. Global minimum analysis of 4DTBP-6,8. The global minimum of 4DTBP-6,8 was searched using CONFLEX. The conformer–energy profile is shown in the panel. Nine samples were extracted from the 1125 conformers, and named samples 1–9. Each sample has two pyridinium rings, and these rings were named as A and B in the holding process.

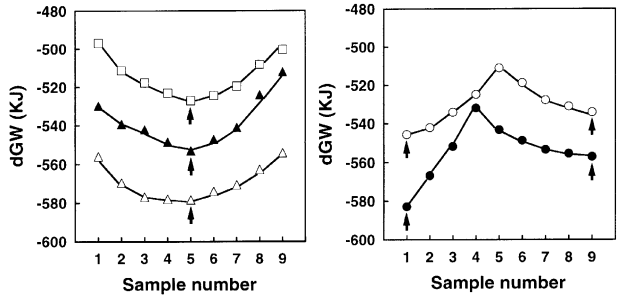

Figure 4. Solvation free energy of 4DTBP-m,8 derivatives. For 4DTBP-6,8, the solvation free energies (dGWs) of nine samples were calculated using MOPAC. The relationship between sample number and dGW is shown in the right panel (open circles). The dGW values of the nine 4DTBP-4,8 samples are shown in the right panel (closed circles). Similarly, the dGWs of 4DTBP-3,8 (open triangles), 4DTBP-8,8 (closed triangles) and 4DTBP-10,8 (open squares) are shown in the left panel.

minimum points (arrow; samples 1 and 9) were observed. Thus two types of hydrophobic 4DTBP-6,8 conformers existed during the holding process. In the 4DTBP-4,8 analysis, 786 conformers were observed; their energy levels were 0.59–11.40 kcal/mol (Fig. 5B). The energy profiles and the holding process of these conformers were similar to those of 4DTBP-6,8 (data not shown). We extracted nine samples (samples 1–9) to calculate the 4DTBP-4,8 dGWs as well as those for 4DTBP-6,8. The correlation between the sample numbers and the dGWs were similar to those of 4DTBP-6,8. Two minimum dGW points were observed (arrow; closed circles in right panel, Fig. 4).

Moreover, we searched the global minimum for other 4DTBP-*m*,8 derivatives, such as 4DTBP-3,8,-8,8,-10,8, and obtained 951 (−1.30 to 9.19 kcal/mol, Fig. 5A), 1587 (−0.21 to 14.44 kcal/mol, Fig. 5C), 2349 (−0.83 to 15.19 kcal/mol, Fig. 5D) conformers. Nine samples were extracted from each derivative as for 4DTBP-6,8, and the solvation free energy (dGW) was calculated. 4DTBP-3,8 had one minimum dGW point (arrow; open triangles in left panel, Fig. 4). Other 4DTBP-m,8 derivatives also had one minimum dGW point arrow in left panel; 4DTBP-8,8 (closed triangles), 4DTBP-10,8 (open squares).

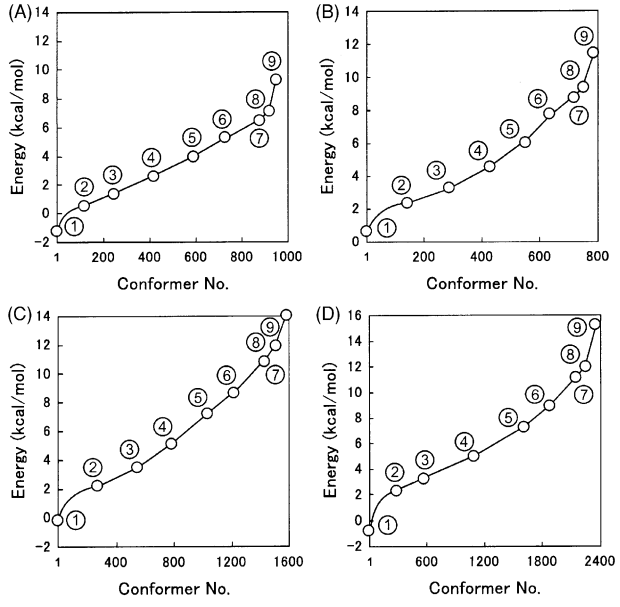

Figure 5. Energy profiles of bis-QACs. The global minimum of 4DTBP-3,8 (A), -4,8 (B), -8,8 (C), -10,8 (D) was searched using CONFLEX as well as for 4DTBP-6,8. Nine samples (1–9) were extracted for solvation free energy (dGW) calculation (Fig. 4).

Acute cytotoxic effect of 4DTBP-*m*,8 derivatives

4DTBP-4,8 and -6,8 had two minimum dGW points (Fig. 4), indicating different cytotoxic profiles to human cells than those of 4DTBP-3,8, -8,8, -10,8. We next examined the acute cytotoxic effect of 4DTBP-*m*,8 for human skin fibroblasts (NB1RGB). 4DTBP-3,8 dose-dependently (20–100 μM) expressed a cytotoxic effect on NB1RGB cells, and reached 100% cytotoxicity at 100 μM (Fig. 6A). 4DTBP-8,8 and -10,8 also indicated a dose-dependent cytotoxicity as did 4DTBP-3,8; 40 μM of these derivatives expressed 100% cytotoxic effect on the NB1RGB cells (Fig. 6D and E).

As shown in Figure 6B, 4DTBP-4,8 gradually expressed cytotoxicity in the range of 20–60 μM, but the toxic effect increased significantly over 60 μM. Both in the

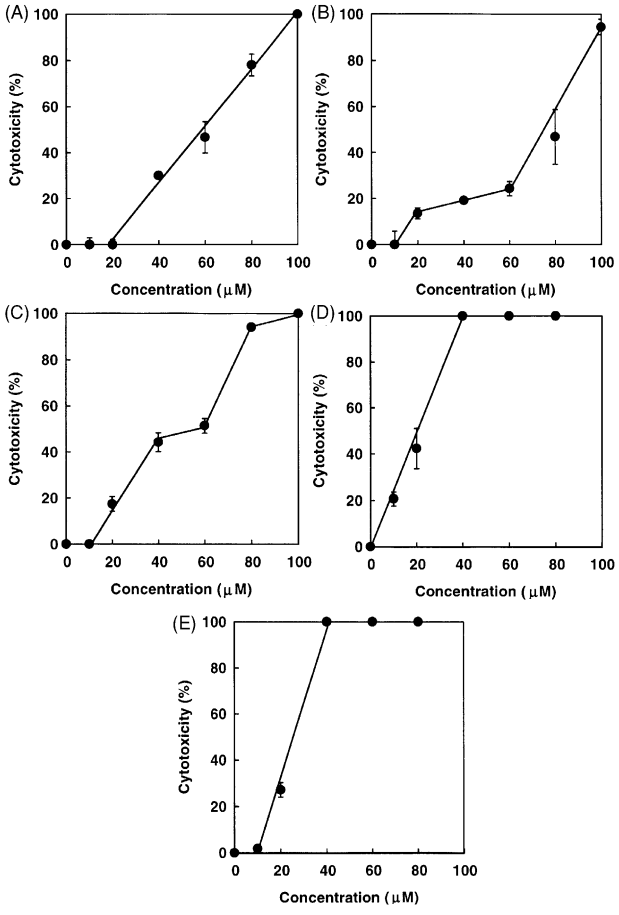

Figure 6. Acute cytotoxicity of 4DTBP-m,8 derivatives on NB1RGB. The cytotoxicity toward human NB1RGB cells was examined. The dose-response curves are shown as follows: 4DTBP-3,8 (A), 4DTBP-4,8 (B), 4DTBP-6,8 (C), 4DTBP-8,8 (D) and 4DTBP-10,8 (E). Results are the mean (±SE) of three determinations.

range of 10–40 and 60–80 μM, 4DTBP-6,8 indicated dose-dependent cytotoxicity (Fig. 6C). Thus these 4DTBP-4,8 and -6,8 derivatives had different cytotoxic profiles on NB1RGB cells than those of other 4DTBP-m,8 derivatives.

Energy profiles of bridge types

We next analyzed the energy–conformer profile of four types of modeled bridge-molecules, which had been examined in the present study. As shown in Fig. 7, the four types of model bridge-molecules (amide type, anti-amide type, ester type, thioether type) were constructed using the CAChe system, and were searched for the global minimum using CONFLEX. The amide type bridge-molecule had 297 conformers (Fig. 7A). The heat of formation energy gradually increased from 31.96 kcal/mol (conformer No. 1) to 33.93 kcal/mol (conformer No. 260), and the energy significantly jumped (arrow) to 38.62 kcal/mol (conformer No. 297). The anti-amide and ester type model molecules had 245 (15.70–23.28 kcal/mol) and 160 (34.45–44.11 kcal/mol) conformers, respectively (Fig. 7B and C). They had energy profiles similar to that of an amide type molecule; energy jump points were observed (arrow in Fig. 7B and C).

In the thioether type model molecule, 241 conformers were obtained by the CONFLEX search. The energy gradually increased from 16.27 kcal/mol (conformer No. 1) to 18.58 kcal/mol (conformer No. 241) (Fig. 7D). Thus the energy profile pattern of a thioether type molecule was different from those of the other three types of model molecules (amide type, anti-amide type, ester type).

Discussion

Previously, we designed and synthesized a series of quaternary ammonium compounds (QACs) with antimicrobial activities and examined their structure–activity relationships.[21–24] 4DTBP-6,8 indicated low cytotoxicity for human cells, and the LD_{50} (Table 1) was almost higher than the minimum inhibitory concentration (MIC) (Table 2). In contrast, the MIC range (4.2–205.0 μM) of benzalkonium chloride (Bz) was above the LD_{50} in all human cells (Table 1). Thus, a Bz cannot be safe antimicrobial agents anytime. 4DTBP-*m*,*n* derivatives had two identical alkylpyridinium rings with an alkyl-chain structure linking the rings to each other by an alkyl-bridge. In the present study, we examined the effect of these alkyl-bridge (*m*) and-chain (*n*) length on the minimum inhibitory concentration (MIC) using *E. coli* K12 W3110. The relationship between the alkyl-bridge length (*m*) and the MIC of 4DTBP-*m*,8 derivatives are shown in Fig. 2F, the MIC became lowest at an alkyl-bridge length of $m=6$. The alkyl-chain length (*n*) affected the antimicrobial activities of bis-QACs, and the MIC on *E. coli* increased following a chain-length dependency (Fig. 2A–E). From these results, we considered that the best combination of alkyl-bridge and chain length to be $m=6$ and $n=8$, respectively. Therefore, 4DTBP-6,8 should be the most useful and safest agent among the present derivatives.

We searched the global minimum of 4DTBP-6,8 using CONFLEX, and obtained 1125 conformers (Fig. 3). Nine samples were extracted from these 1125 conformers in order of the energy (kcal/mol) level. As

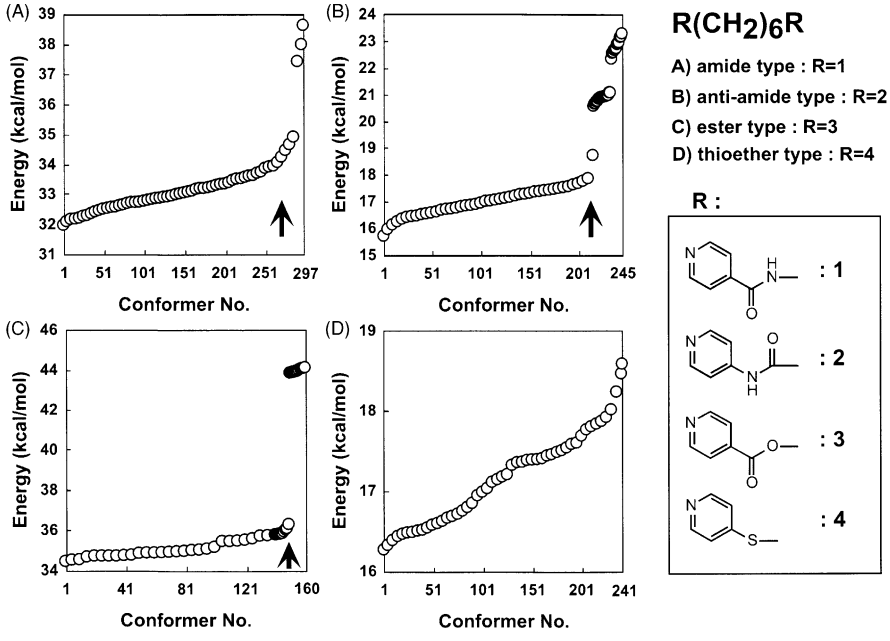

Figure 7. Energy profiles of model bridge-molecules. The global minimum of four bridge-type molecules were analyzed. The energy–conformer profiles are shown as follows: (A), amide type; (B), anti-amide type; (C), ester type; (D), thioether type. Chemical structures of these model molecules are shown in the right panel.

shown in Figure. 3, these nine samples (samples 1–9) could be regarded as the holding process. In general, hydrophobicity is one of the important factors for pharmaceutical activities. The solvation free energy (dGW) is concerned with hydrophobicity. We have examined the relationship between dGW and biological activity in drug design.[26,27] The dGW value was defined as free-energy changes for association in a vacuum (dGWv) and in aqueous solution (dGWw) using molecular orbital calculations (dGW = dGWw − dGWv).[25] In the dGW analysis of 4DTBP-6,8, two minimum dGW points were observed (open circles in Fig. 4 right panel). We considered that two different types of 4DTBP-6,8 conformers existed, which had the same degree of hydrophobicity (samples 1 and 9 in Fig. 3). Because hydrophobicity should be related to association with the cell membrane, we predicted that 4DTBP-6,8 had two types of conformer-involved activity (e.g., cytotoxicity). Indeed, 4DTBP-6,8 showed two break-points (at 40 and 60 μM) in cytotoxic effect on human NB1RGB cells (Fig. 6C).

We also performed the global minimum search for 4DTBP-3,8, -4,8, -8,8, -10,8 derivatives, and obtained 951, 786, 1589, 2349 conformers, respectively (Fig. 5). For each derivative, we extracted nine samples (samples 1–9) from these conformers as for 4DTBP-6,8, and calculated the dGW values (Fig. 4). Two minimum dGW points were observed in the 4DTBP-4,8 analysis as well as for 4DTBP-6,8 (arrow; closed circles in Fig. 4 right panel). On the other hand, 4DTBP-3,8 (open triangles),-8,8 (closed triangles), -10,8 (open squares) derivatives had one minimum dGW point (left panel in Fig. 4); thus the existence of one hydrophobic conformer should be expected for these derivatives. From these results, we considered that 4DTBP-m,n derivatives should be divided into two groups (group 1: 4DTBP-4,8, -6,8; group 2: 4DTBP-3,8, -8,8, -10,8), and we expected that each group would have distinctive activity to human cells (e.g., cytotoxicity, hemolysis). Indeed, 4DTBP-3,8,-8,8, -10,8 showed a cytotoxic activity dose-dependence toward NB1RGB cells, while 4DTBP-4,8 and -6,8 had a non-linear cytotoxicity (Fig. 6). Therefore, we considered that the excellent balance between antibacterial activity and the safety of 4DTBP-6,8 was dependent upon a delicate hydrophobicity, which was predicted from the dGW analysis. The human cell membrane and bacterial cell membrane (or wall) should have different features. Then it should be very important to consider the affinity of them to antibacterial drugs. Now, we are examining the relationship between the antibacterial activity and the binding ability to cell membrane (or wall) of 4DTBP-*m*,*n* derivatives.

The bridge portion in bis-quaternary ammonium compounds (bis-QACs) had been analyzed using model molecules, and conformer-energy profiles obtained (Fig. 7). In thioether type model bridge-molecule, the energy gradually increased from conformer 1 (global minimum) to conformer 241 (Fig. 7D). The other (amide, anti-amide, ester) types indicated an energy jump as shown in Figure 7A–C. We considered that the bridge feature (e.g., flexibility) of these bis-QACs should be related to the balance between antibacterial activity and safety. We are now examining the effect of bridge feature both on antibacterial activity and cytotoxicity.

Experimental

Reagents

Reagents used were as follows: 1-methoxy-5-methylphenazinium methylsulfate (PMS), 2-(4-indophenyl)-3-(4-nitrophenyl)-5-(2,4-disulfophenyl)-2H-tetrazolium monosodium salt (WST-1), Dojindo Lab., Kumamoto, Japan. PMS/WST-1 solution was prepared for use as follows: 25 μL of 0.2 mM PMS aqueous solution was mixed with 1.225 mL of 20 mM sodium 2-[4-2(-hydroxyethyl)-1-piperazinyl]ethanesulfate (HEPES) buffer (pH 7.4); then 4.1 mg of WST-1 was added to the mixture and dissolved completely.

The structure of antibacterial agents (bis-QACs) are as follows (Fig. 1); (1) amide type: *N,N′* - tetramethylenebis(1-dodecyl-4-carbamoylpyridinlum iodide (4BCAP-4,12), *N,N′*-hexamethylenebis(1-decanyl-4-carbamoylpyridinium iodide (4BCAP-6,10), (2) anti-amide type: 4,4′-(1,4-tetramethylenedicarbonyldiamine)bis(1-decylpyridinium iodide) (4DCABP-4,10), 4,4′-(1,4-tetramethylenedicarbonyldiamine)bis(1 - dodecylpyridinium iodide) (4DCABP-4,12), 4,4′-(1,4-phenyldicarbonyldiamine)bis(1-dodecylpyridinium iodide) (4DCABP-P,12), (3) ester type: 4,4′-(1,6-hexamethylenedioxydicarbonyl)-bis(1-dodecylpyridinium iodide) (4DOCBP-6,12), (4) thioether type: 4,4′-(1,6-hexamethylenedithio)bis(1-octylpyridinium iodide) (4DTBP-6,8) and (5) monomer type (benzalkonium chloride). These bis-QACs were synthesized in our laboratory.[21,22] These QACs were dissolved in saline, sterilized by filtration through 0.22 micro-meter pore size membrane and stored at −30 °C until use except for the ester type bis-QAC, 4DOCBP-6,12. The solution of 4DOCBP-6,12 was freshly prepared for use. The elemental analyses of bis-QACs were summarized in Table 3.

Acute phase cytotoxic assay. The acute phase cytotoxic assay using human cells (NHEK(F), NB1RGB, erythrocyte, JM) was carried out as following. The NHEK(F) and NB1RGB were suspended in each maintaining medium and dispensed into the wells of a 96-multiwell culture plate 100 μL/well at 5.0×10^4 cells/well condition. When cell density reached to confluence, each 50 μL of the supernatant was replaced with 50 μL of a mixture of 1 volume of phosphate buffered saline (PBS) containing bis-QAC and 4 volumes of the fresh maintaining medium and incubated at 37 °C for 1 h. Then, 10 μL of the mixture solution of PMS and WST-1 was added to each well and incubated for 1 h to produce a water-soluble formazan.[28] Finally, the cell death (%) was calculated by measuring the absorbance at 415 nm indicating the mitochondrial activity using a Bio-Rad model550 microplate reader. Saline or 1 (v/v)% SDS solution

Table 3. Elemental analyses of synthesized bis-QACs[a]

Compd	Elemental analyses (%)			Mp (°C)	Yield (%)
	H calcd (found)	C calcd (found)	N calcd (found)		
4BCAP-4,12	7.69(7.55)	53.93(53.98)	6.29(6.45)	155–157	5.0
4BCAP-6,10	7.48(7.37)	52.90(52.60)	6.49(6.50)	97–99	29.4
4DCABP-4,10	7.25(7.03)	51.80(51.82)	6.71(7.00)	188—190	29.8
4DCABP-4,12	7.69(7.57)	53.93(53.89)	6.29(6.09)	206—208	33.0
4DCABP-P,12	7.90(7.77)	61.76(61.73)	6.86(6.84)	255—258	84.2
4DOCBP-6,12	7.66(7.36)	54.78(54.75)	3.04(3.09)	165—167	60.5
4DTBP-6,8	6.94(6.80)	48.98(48.93)	3.57(3.57)	102—103	88.0
4DTBP-3,8	6.51(6.25)	46.90(46.81)	3.77(3.51)	125—128	80.5
4DTBP-3,10	7.07(6.94)	49.62(49.43)	3.51(3.78)	159—161	81.2
4DTBP-3,12	7.55(7.29)	51.99(51.87)	3.28(2.99)	169—170	80.3
4DTBP-3,14	7.97(7.77)	54.06(53.78)	3.08(2.93)	174—175	82.1
4DTBP-3,16	8.34(8.04)	55.89(55.80)	2.90(2.98)	166—169	83.4
4DTBP-3,18	8.67(8.33)	57.52(57.25)	2.74(2.71)	149—151	85.0
4DTBP-4,8	6.66(6.53)	47.62(47.37)	3.70(4.00)	147—149	80.0
4DTBP-4,10	7.19(6.96)	50.24(49.95)	3.45(3.40)	149—151	81.2
4DTBP-4,12	7.66(7.38)	52.53(52.34)	3.22(3.01)	168—171	80.7
4DTBP-4,14	8.06(8.00)	54.54(54.31)	3.03(3.02)	165—168	80.5
4DTBP-4,16	8.42(8.21)	56.31(56.08)	2.86(3.12)	175—178	83.2
4DTBP-4,18	8.75(8.50)	57.90(57.65)	2.70(2.66)	165—168	84.2
4DTBP-6,10	7.43(7.28)	51.42(51.54)	3.33(3.39)	121—122	87.2
4DTBP-6,12	7.87(7.63)	53.56(53.47)	3.12(3.09)	136—137	87.3
4DTBP-6,14	8.25(7.96)	55.45(55.15)	2.94(2.74)	135—136	86.5
4DTBP-6,16	8.59(8.41)	57.13(57.06)	2.78(2.77)	140—141	86.8
4DTBP-6,18	8.89(8.97)	58.63(58.38)	2.63(2.40)	138—139	87.0
4DTBP-8,8	7.19(7.07)	50.24(49.96)	3.45(3.74)	87–89	84.3
4DTBP-8,10	7.66(7.57)	53.53(52.32)	3.22(3.09)	122–123	83.2
4DTBP-8,12	8.06(7.85)	54.54(54.31)	3.03(2.73)	132–133	86.5
4DTBP-8,14	8.42(8.27)	56.31(56.01)	2.86(3.11)	137–138	84.6
4DTBP-8,16	8.75(8.55)	57.90(57.68)	2.70(2.65)	148–149	83.5
4DTBP-8,18	9.03(8.73)	59.32(59.15)	2.56(2.49)	155–157	84.0
4DTBP-10,8	7.43(7.17)	51.42(51.12)	3.33(3.18)	119–120	82.1
4DTBP-10,10	7.87(7.84)	53.56(53.43)	3.12(3.36)	128–129	82.6
4DTBP-10,12	8.25(8.10)	55.45(55.15)	2.94(3.22)	134–136	84.6
4DTBP-10,14	8.59(8.33)	57.13(56.86)	2.78(2.56)	142–144	85.3
4DTBP-10,16	8.89(8.65)	58.63(58.65)	2.63(2.54)	148–149	85.6
4DTBP-10,18	9.17(8.95)	60.00(59.76)	2.50(2.39)	152–154	85.6

[a]The lower panel summarized elemental analyses of 4DTBP-6,8 derivatives.

were used instead of the medium/QAC mixture to estimate the cell death of the background level or of the full level, respectively. The cytotoxicity (cell death; %) was estimated as follows: Cell death (%) = [(A_{415} measured in the absence of QAC) − (A_{415} measured in the presence of QAC)]/[(A_{415} measured in the absence of QAC) − (A_{415} measured in the presence of 1(v/v)%SDS)] × 100.

JM culture (90 μl) (1.0×10^6 cells/mL) was mixed with 10 μL of the QAC solution in a microcentrifuge tube and incubated at 37 °C for 1 h. For estimating the background cell death level, 10 μL of saline was used instead of the QAC solution. After incubation, 100 μL of saline containing 0.4% Trypan blue was added, and a portion of the final mixture was transferred onto the hemocytometer. The cytotoxicity was estimated by means of Trypan blue exclusion using the following equation: Cytotoxicity (%) = [(number of Trypan blue-stained cells in the present of QAC/number of total cells in the present of QAC) − (number of Trypan blue-stained cells in the absence of QAC/number of total cells in the absence of reagent)] × 100.

The assay for the acute phase cytotoxic effect of QACs on erythrocytes, hemolysis assay, was performed as described previously.[29] Briefly, 990 μL of PBS containing QAC was mixed with 10 μL of 50(v/v)% normal human erythrocytes suspension in a microcentrifuge tube and incubated at 37 °C for 1 h. After the reaction, each tube was centrifuged for 5 min at 3000 rpm in a Kubota model 1900 microcentrifuge at 4 °C. Absorbance at 540 nm of each supernatant was measured in a Hitachi model U-2000 spectrophotometer. Assay in just PBS and in distilled water without QAC were carried out for estimation of the background hemolysis and the full hemolysis, respectively.

The LD_{50} value was defined as the concentration of each reagent giving 50 % cell death. It was calculated using the following equation: log[(cell death % in the presence of QAC − cell death % of the background level)/(cell death % of the full level − cell death % in the presence of QAC)] = a ($\log LD_{50} - \log[QAC]$). a, a constant depending on each cell system and reagents. The LD_{50} value will be given when the left term in the equation is zero.

Bacteriostatic activity. The minimal inhibitory concentration (MIC) was measured according to a standard dilution method described previously[11] using a bacterial strain panel consisting of *Pseudomonas aeruginosa* ATCC27583, ATCC10145 and IFO3080, *Klebsiella pneumoniae* ATCC4352 and ATCC13883, *Proteus rettgeri* NIH96, *Proteus vulgoris* ATCC13315, *Proteus mirabilis* IFO3849, *Escherichia coli* K12 OUT 8401 and K12 W3110, *Bacillus subtilis* IFO3134 and ATCC6633, *Bacillus cereus* IFO3001, *Micrococcus luteus* IFO12708, *Staphylococcus aureus* IFO12732 and JC1(MRSA), respectively.

Global minimum analysis and solvation free energy calculation for 4DTBP-*m*,8 derivatives. The initial structure of 4DTBP-6,8 was constructed using CAChe (Fujitsu Ltd., Japan). The global minimum analysis of 4DTBP-6,8 was performed using CONFLEX with MM2 forcefield (Fujitsu Ltd., Japan), and 1125 conformers were obtained. Nine conformers (samples 1–9) were extracted from these 1125 conformers. The calculated three-dimensional structures of nine samples and the energy–conformer profile are shown in Figure 3. The 3-D-projected view of the calculated conformers were drawn by ORTEP-III (Dr. L. J. Farrugia, University of Glasgow, 1996).

The solvation free energy (dGW) of nine conformers (samples 1–9) were calculated using MOPAC (Fujitsu Ltd., Japan) as described previously.[25–27] The energy calculations were performed with the PM3Hamiltonian using MOPAC; the stable transient structures were initially built with general parameters of bond length, bond angle, and dihedral angle, and refined with the eigen-vector following (EF) optimization methods.

For 4DTBP-3,8, -4,8, -8,8, -10,8 derivatives, the nine samples were obtained using CONFLEX as well as for 4DTBP-6,8. The dGW values were calculated by MOPAC.

Analysis of four types of the model bridge-molecules. The bridge region of four types of bis-quaternary ammonium compounds [$R(CH_2)_6R$, Fig. 7] were modeled using CAChe (Fujitsu Ltd., Japan). Their global minimum analysis was performed using CONFLEX with the MM3 forcefield, thus obtaining the conformer–energy profiles.

Acknowledgements

This work was supported, in part, by Grant-in-Aid for Scientific Research (15590098) from the Ministry of Education, Science, Sports and Culture, Japan.

References and Notes

1. Augustin, C.; Damour, O. *Cell Biol. Toxicol.* **1995**, *11*, 167.
2. Damour, O.; Hua, S. Z.; Lasne, F.; Villain, M.; Rousselle, P.; Collombel, C. *Burns* **1992**, *18*, 479.
3. Steinsvag, S. K.; Bjerknes, R.; Berg, O. H. *Acta Oto-laryngol.* **1996**, *116*, 868.
4. Tripathi, B. J.; Tripathi, R. C. *Lens Eye Toxicity Res.* **1989**, *6*, 395.
5. Kourai, H.; Hasegawa, Y.; Goto, S.; Nakagawa, K. *J. Antibact. Antifungal Agents* **1994**, *22*, 461.
6. Kourai, H.; Hasegawa, Y.; Wada, K. *J. Antibact. Antifungal Agents* **1994**, *22*, 653.
7. Kourai, H.; Takechi, H.; Horie, T.; Uchiwa, N.; Takeichi, K.; Shibasaki, I. *J. Antibact. Antifungal Agents* **1985**, *13*, 3.
8. Kourai, H.; Takeichi, H.; Horie, T.; Takeichi, K.; Shibasaki, I. *J. Antibact. Antifungal Agents* **1985**, *13*, 245.
9. Kourai, H.; Takechi, H.; Kume, M.; Takeichi, K.; Shibasaki, I. *J. Antibact. Antifungal Agents* **1986**, *14*, 55.
10. Kourai, H.; Takechi, H.; Muramatsu, K.; Shibasaki, I. *J. Antibact. Antifungal Agents* **1989**, *17*, 119.
11. Okazaki, K.; Maeda, T.; Nagamune, H.; Kourai, H. *Biocontrol Sci.* **1997**, *2*, 39.
12. Okazaki, K.; Maeda, T.; Nagamune, H.; Kourai, H. *Jpn. J. Toxicol. Environ. Health* **1998**, *43*, 251.
13. Kourai, H.; Machikawa, F.; Tateishi, K.; Horie, T.; Takeichi, K.; Shibasaki, I. *J. Antibact. Antifungal Agents* **1983**, *11*, 553.
14. Kourai, H.; Manabe, Y.; Matsutani, E.; Hasegawa, Y.; Nagagawa, K. *J. Antibact. Antifungal Agents* **1995**, *23*, 271.
15. Kourai, H.; Machikawa, F.; Horie, T.; Takeichi, K.; Shibasaki, I. *J. Antibact. Antifungal Agents* **1983**, *11*, 51.
16. Devinsky, F.; Lacko, I.; Bittererova, F.; Tomeckova, L. *J. Colloid Interface Sci.* **1986**, *114*, 314.
17. Okazaki, K.; Manabe, Y.; Maeda, T.; Nagamune, H.; Kourai, H. *Biocontrol Sci.* **1996**, *1*, 51.
18. Maeda, T.; Goto, S.; Manabe, Y.; Okazaki, K.; Nagamune, H.; Kourai, H. *Biocontrol Sci.* **1996**, *1*, 41.
19. Devinsky, F.; Lacko, I.; Mlynarcik, D.; Racansky, V.; Krasnec, L. *Tenside Deterg.* **1985**, *22*, 10.
20. Pavlikova, M. M.; Lacko, I.; Devinsky, F.; Masarova, L.; Mlynarcik, D. *Folia Microbiol.* **1994**, *39*, 176.
21. Okazaki, K.; Maeda, T.; Nagamune, H.; Manabe, Y.; Kourai, H. *Chem. Pharm. Bull.* **1997**, *45*, 1970.
22. Maeda, T.; Okazaki, K.; Nagamune, H.; Manabe, Y.; Kourai, H. *Biol. Pharm. Bull.* **1998**, *21*, 1057.
23. Gsll, D.; Knight, P. A.; Hampson, F. *Immunology* **1972**, *23*, 569.
24. Nagamune, H.; Maeda, T.; Ohkura, K.; Yamamoto, K.; Nakajima, M.; Kourai, H. *Toxicol. Vitro* **2000**, *14*, 139.
25. Ohkura, K.; Hori, H. *Bioorg. Med. Chem.* **1999**, *7*, 309.
26. Zhu, J. W.; Nagasawa, H.; Nagura, F.; Mohamad, S. B.; Uto, Y.; Ohkura, K.; Hori, H. *Bioorg. Med. Chem.* **2000**, *8*, 455.
27. Hori, H.; Nagasawa, H.; Ishibashi, M.; Uto, Y.; Hirata, A.; Saijo, K.; Ohkura, K.; Kirk, K. L.; Uehara, Y. *Bioorg. Med. Chem.* **2002**, *10*, 3257.
28. Ishimura, M.; Mizoguchi, M.; Shiga, M.; Sasamoto, K. *Chem. Pharm. Bull.* **1993**, *41*, 1118.
29. Nagamune, H.; Ohnishi, C.; Katsuura, A.; Fushitani, K.; Whiley, R. A.; Tsuji, A.; Matsuda, Y. *Infect. Immun.* **1996**, *64*, 3093.